COMBINATION OF COMPRESSED SENSING AND PARALLEL IMAGING FOR HIGHLY-ACCELERATED DYNAMIC MRI

Ricardo Otazo, Li Feng, Hersh Chandarana, Tobias Block, Leon Axel, Daniel K. Sodickson

Bernard and Irene Schwartz Center for Biomedical Imaging
Department of Radiology, NYU School of Medicine
New York, NY, USA

ABSTRACT

The introduction of compressed sensing methods to speed up image acquisition has received great attention in the Magnetic Resonance Imaging (MRI) community. Compressed sensing exploits the compressibility of medical images to reconstruct unaliased images from undersampled data. Moreover, compressed sensing can be synergistically combined with previously introduced acceleration methods such as parallel imaging, which employs arrays of receiver coils to further increase imaging speed. Over the past three years, we have been working on the combination of compressed sensing and parallel imaging, exploiting the idea of joint multicoil sparsity. In this work, we present a summary of our image acquisition and reconstruction methods for the combination of compressed sensing and parallel imaging, and describe applications to cardiac and body dynamic MRI.

Index Terms— Compressed sensing, parallel imaging, dynamic MRI, cardiac imaging, body imaging

1. INTRODUCTION

Magnetic Resonance Imaging (MRI) provides several advantages as compared with other imaging modalities, such as superior soft-tissue characterization, absence of ionizing radiation and flexible image contrast. However, a major limitation is the relatively slow imaging speed, which limits temporal and spatial resolution and volumetric coverage, and introduces motion related artifacts. In dynamic imaging, where a time-series of images is acquired to create a movie of organ function or to follow the passage of a contrast agent, spatial resolution and volumetric coverage are usually sacrificed in order to maintain an adequate temporal resolution and reduce motion-related artifacts.

Compressed sensing (CS) [1-3] has recently emerged as a powerful rapid imaging approach, exploiting image compressibility, which promises to revolutionize MRI and change the way we think about imaging. Instead of acquiring a fully-sampled image and compressing it afterwards (standard compression), CS takes advantage of the fact than an image is usually sparse in some appropriate basis and reconstructs this sparse representation from undersampled data, without loss of important information. Successful application of CS requires image sparsity and incoherent measurements. Dynamic MRI is a good candidate for CS, due to (a) extensive correlations between image frames which typically result in sparse representations after applying an appropriate temporal transform, such as FFT, Principal Component Analysis (PCA) or finite differences (which is equivalent to total variation (TV) minimization), and (b) the possibility of using a different random undersampling pattern for each temporal frame, which increases incoherence and distributes the incoherent aliasing artifacts along the temporal dimension resulting in artifacts with lower intensity

CS can be combined with parallel imaging (PI) to further increase imaging speed. PI is a well-established acceleration technique that employs multiple receiver coils with different spatial sensitivities to reconstruct images from regularly undersampled k-space data [4-6]. We have developed combinations of CS and PI, using the idea of joint multicoil sparsity, which have resulted in acceleration rates not previously feasible for dynamic MRI techniques [7-9].

This work aims to describe our experience with the combination of CS and PI for highly accelerated dynamic MRI. First, we describe the general methodology for image acquisition and reconstruction using Cartesian and radial trajectories, and then we demonstrate the performance of the combined approach in cardiac and body dynamic MRI examples.

2. COMBINATION OF COMPRESSED SENSING AND PARALLEL IMAGING

2.1. General Description

To synergistically combine CS and PI, we have developed a joint CS reconstruction that enforces joint sparsity on the multicoil model instead of performing separate CS reconstructions for each coil [7]. Using this approach, the additional spatial encoding capabilities of multiple receiver coils can be exploited to reduce the incoherent aliasing artifacts in the multicoil combination and thus enable higher acceleration rates. Figure 1 shows the reduction of incoherent aliasing artifacts when considering a joint 4-coil planar array model compared to a single coil model.

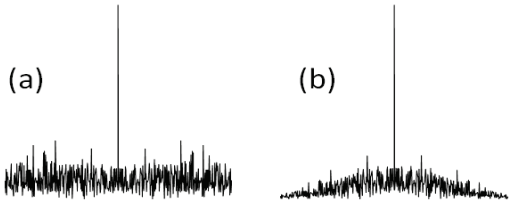


Figure 1: Point spread function corresponding to 4-fold random undersampling for (a) single coil system and (b) 4-coil system.

The formulation of the combination of CS and PI assumes that the acquired k-space data for each coil is given by:

$$y_l = FS_l x, \tag{1}$$

where F is the spatial Fourier transform, S_l is the coil sensitivity and x is the image to reconstruct. The multicoil model is formed by concatenating the individual models:

$$y = Fx, \tag{2}$$

where $y = \begin{bmatrix} y_1 \\ \vdots \\ y_{Nc} \end{bmatrix}$, $E = F\begin{bmatrix} S_1 \\ \vdots \\ S_{Nc} \end{bmatrix}$, and N_c is the number of coils. The joint CS reconstruction is given by:

$$\min\|Wx\|_1 \text{ subject to } \|Ex - y\|_2 < \varepsilon \tag{3}$$

where W is the sparsifying transform, $\|.\|_p$ is the p-norm and ε is the model error threshold (usually set to the noise level). The l_1-norm term enforces joint multicoil sparsity, since x represents the contributions from all coils, and the l_2-norm term enforces multicoil data consistency. For CS alone or coil-by-coil CS, the number of required k-space samples is about 3 to 5 times the number of sparse coefficients. However, for joint CS & PI, only about the number of sparse coefficients is required for arrays with very large number of coils, which approximates the ideal case for l_0-norm minimization [l0].

2.2. Cartesian vs. Radial k-Space Trajectories

Random undersampling patterns are required for Cartesian k-space trajectories to produce the required incoherent aliasing artifacts. However, in Cartesian trajectories, only phase-encoding dimensions can be undersampled to increase imaging speed, which limits the performance of compressed sensing. Radial trajectories are an attractive alternative for compressed sensing, due to the inherent presence of incoherent aliasing artifacts in multiple dimensions, even for regular undersampling, which enables us to exploit additional sparsity and incoherence along frequency-encoding dimensions. It is also known that radial trajectories are less sensitive to motion, allowing for better performance in capturing dynamic information. Furthermore, the use of golden-angle acquisition schemes in dynamic radial MRI, where uniform coverage of k-space is obtained by grouping consecutive spokes, further increases incoherence and allows for continuous data acquisition and reconstruction with arbitrary temporal resolution at arbitrary time points.

2.3. Practical Implementation

We have developed two methods for the combination of CS and PI: (a) k-t SPARSE-SENSE [7], which uses random undersampling of Cartesian trajectories, and (b) Golden-angle Radial Sparse Parallel MRI (GRASP) [11], which uses continuous acquisition of radial spokes with golden-angle scheme and allows reconstruction with arbitrary temporal resolution. The golden-angle scheme uses an increment of 111.25° for consecutive radial spokes, which enables uniform k-space coverage by grouping a specific number of spokes. GRASP continuously acquires data for a certain period of time and then creates the different temporal frames by grouping together consecutive radial spokes. Usually, a few spokes (8-13) are enough for each temporal frame to obtain good image quality, resulting in very high accelerations. Figure 2 shows the data acquisition schemes for k-t SPARSE-SENSE and GRASP. k-t SPARSE-SENSE reconstruction employs the FFT along the spatial dimensions as the operator F in Eq. (1) and (2). For GRASP, F is given by the Non-Uniform FFT (NUFFT) [12] operator (which was previously used to reconstruct non-Cartesian k-space data). We have implemented two algorithms that solve Eq. (3): (a) non-linear conjugate gradient and (b) soft-thresholding. The non-linear conjugate gradient method is an extension of the algorithm presented in [3] to enforce joint multicoil sparsity. It aims to minimize the following objective function:

$$D(x) = \|Ex - y\|_2 + \lambda \|Wx\|_1 \tag{4}$$

where λ is a regularization parameter that controls the tradeoff between sparsity and data consistency. Instead of trying to find the optimal λ for each case, we have obtained similar results by decreasing λ during the iterations.

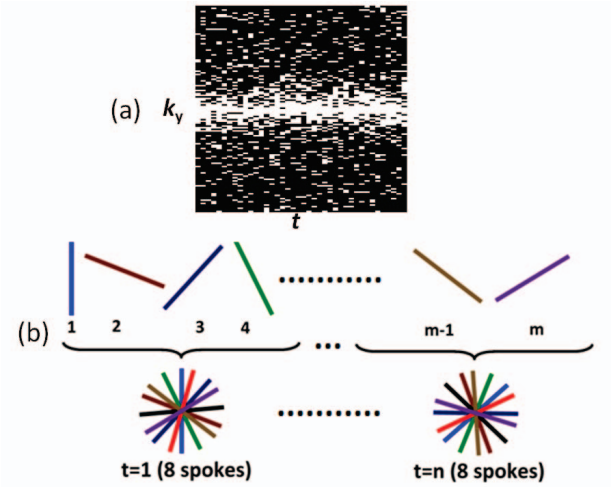


Figure 2: Data acquisition schemes for (a) k-t SPARSE-SENSE: different k_y random undersampling pattern on a Cartesian k-space grid for each temporal frame (white: sampled) and (b) GRASP: continuous acquisition of radial spokes with golden-angle separation. The temporal frames in k-t SPARSE-SENSE are predefined, while GRASP offers the flexibility of arbitrary temporal resolutions by grouping a different number of consecutive frames.

The iterative soft-thresholding algorithm uses the following steps for each iteration:

1. Threshold in the sparse domain: $x_i = W^H S(W x_{i-1}, \lambda)$, where ^{H} is the conjugate transpose, $S(.)$ is the soft-thresholding operator: $S(x,\lambda) = \begin{cases} \frac{x}{|x|}(|x| - \lambda), |x| > \lambda \\ 0, \text{otherwise} \end{cases}$
2. New k-space: $z_i = E x_i$
3. Data consistency: $y_i(k) = \begin{cases} y(k), \text{if k was sampled} \\ z_i(k), \text{otherwise} \end{cases}$
4. Reconstructed image: $x_i = E^H y_i$

The iterative soft-thresholding method enforces true data consistency, updating only the missing k-space points, at the expense of slightly higher noise amplification than the non-linear conjugate gradient algorithm.

3. APPLICATION TO DYNAMIC MRI

2.1. Cardiac Perfusion MRI

Our first application was first-pass cardiac perfusion MRI, a promising and much-studied modality for non-invasive assessment of coronary artery disease, which suffers in a particularly acute fashion from temporal constraints in its need to follow the contrast passage. A T_1-weighted TurboFLASH pulse sequence was modified to include a different random undersampling along the phase encoding dimension (k_y) for each time point (t). The k-t SPARSE-SENSE method was employed to reconstruct the undersampled data using a temporal FFT as sparsifying transform. Figure 3 shows the reconstruction of data acquired with 8-fold acceleration on a 3T Siemens Tim Trio scanner using a standard 12-element matrix coil array. The relevant imaging parameters include: FOV = 320×320mm^2, slice-thickness = 8mm image matrix size = 192×192, spatial resolution = 1.67×1.67mm^2, TE/TR = 1.3/2.5ms, and temporal resolution = 60ms. The reconstructed images covered most of the heart (10 slices were feasible) with adequate contrast enhancement and good image quality. These results represent a considerable improvement over standard parallel imaging, which can only acquire 2-3 slices with the same spatial resolution.

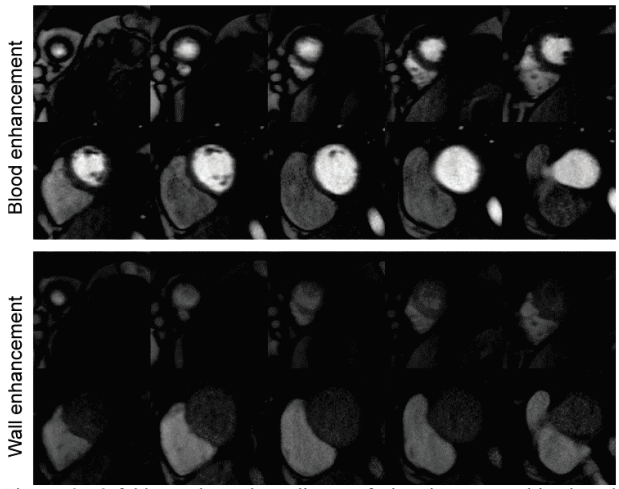


Figure 3: 8-fold accelerated cardiac perfusion images at blood and myocardial wall enhancement phases using k-t SPARSE-SENSE. The technique enabled whole-heart coverage with temporal resolution of 60ms/slice and in-plane resolution of less than 2mm.

2.2. Cardiac Cine MRI

Cardiac cine MRI is a valuable technique for assessment of myocardial function. Cine techniques must deal with the challenge of respiratory motion, particularly in patients who cannot hold their breath. We have developed free-breathing 2D cine within a single heartbeat and whole-heart 3D cine within a single breath-hold using the GRASP technique with temporal TV as sparsifying transform. A Steady State Free Precession (SSFP) pulse sequence with radial sampling using the golden-angle scheme was employed for data acquisition on a 1.5T Siemens Avanto scanner equipped with the standard 12-element matrix coil array. For 2D cine, 500 continuous spokes were acquired during 1.5sec and groups of 8 consecutive spokes were used to form a temporal frame, resulting in a temporal resolution of 20.8ms (50fps). The relevant parameters for 2D cine were FOV = 400×400mm^2, slice-thickness = 10mm image matrix = 192×192, spatial resolution = 2×2mm^2, TE/TR = 2.6/1.3ms. For 3D cine, a stack-of-stars trajectory (radial along k_y-k_x and Cartesian along k_z) was employed. For each partition, 320 spokes were acquired during each heartbeat for a total of 30 heartbeats and 8 consecutive spokes were employed to form a temporal frame (acquisition window = 22.4 ms). The relevant parameters for 3D cine were image matrix = 192×192×40, spatial resolution = 2×2×3mm^2, TE/TR = 2.8/1.4ms. Figure 4 shows reconstruction results with good image quality for free-breathing 2D cardiac cine and whole-heart 3D cine within a single breath-hold using GRASP.

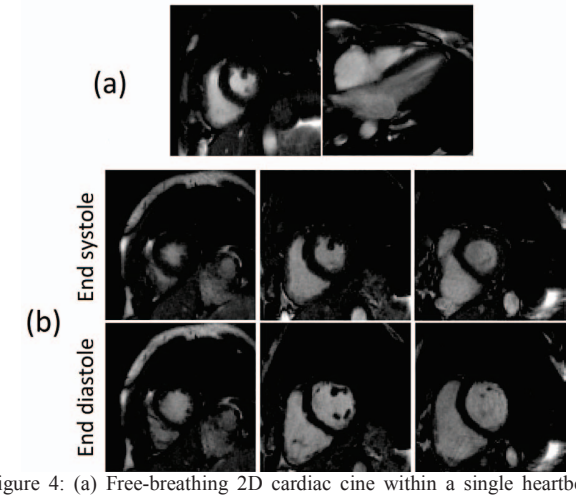


Figure 4: (a) Free-breathing 2D cardiac cine within a single heartbeat with a temporal resolution of 50fps for short axis (left) and long axis (right) views using GRASP with 8 spokes / frame. (b) 3D cardiac cine within a single breath-hold for three different slices at end-diastole and end-systole cardiac phases using GRASP with 8 spokes / frame.

2.3. Contrast-Enhanced Liver MRI

Assessment of multi-phase (arterial and venous) post-contrast acquisition is essential for liver lesion detection and characterization. Image quality, as well as temporal and spatial resolution, are limited by the breath-hold capability of the patient. Inadequate breath-hold capacity results in temporal and spatial blurring, limiting the ability to detect small lesions. The use of radial trajectories without compressed sensing enabled free-breathing scans, at the expense of reduced temporal resolution compared to breath-held Cartesian scans [13]. We have developed a highly-accelerated free-breathing 3D contrast-enhanced liver MRI technique with high spatial and temporal resolution, using GRASP with temporal TV as sparsifying transform. A 3D stack-of-stars (radial sampling for k_y-k_x and Cartesian sampling for k_z) FLASH pulse sequence with golden-angle scheme was employed on a whole-body 3T Siemens Verio scanner equipped with a 12-coil body matrix array. Relevant imaging parameters include: FOV = 380×380 mm2, base resolution = 384 for each radial spoke, slice thickness = 3 mm, TE/TR = 1.7/3.9 ms. 600 spokes were continuously acquired for each of 30 slices during free-breathing, to cover the entire liver; the total acquisition time was 77 seconds. 13 consecutive spokes were employed to form each temporal frame, resulting in a temporal resolution of 1.5 sec. The reconstructed 3D image matrix for each temporal frame was 384×384×30 with a spatial resolution of 1×1×3 mm3. Figure 5 shows reconstruction results at arterial and portal vein peak enhancement for two selected slices. The images yielded appropriate contrast enhancement with good image quality, despite the high acceleration employed.

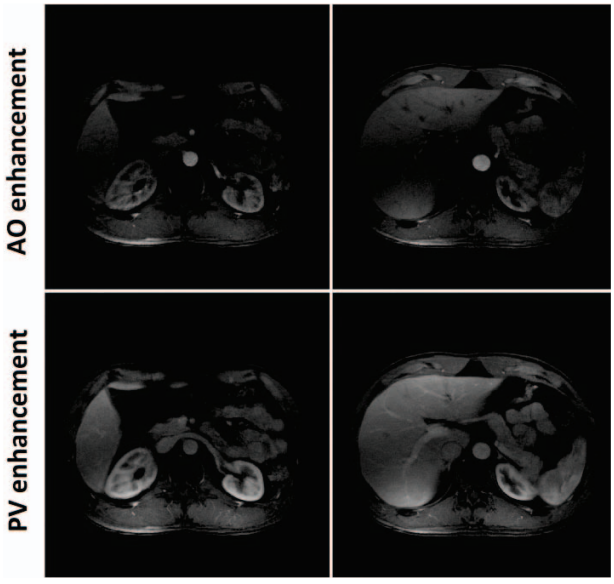


Figure 5: Free-breathing 3D dynamic liver imaging using GRASP in two selected slices at arterial (AO) and portal vein (PV) peak enhancements. Only 13 radial spokes were employed to reconstruct each temporal frame (384 spokes) resulting in a temporal resolution of about 1.5 sec to image the entire liver with a spatial resolution of 1×1×3 mm^3 .

4. CONCLUSIONS

The combination of compressed sensing and parallel imaging enables previously inaccessible combinations of temporal resolution, spatial resolution and volumetric coverage in dynamic MRI by jointly exploiting image sparsity and coil sensitivity encoding. Improved performance is expected with the development of new sparsifying transforms, highly incoherent non-Cartesian sampling and the use of coil arrays with a large number of elements. Our simple and effective methods demonstrated great value for cardiac and body imaging, and they can be used to improve other current clinical techniques and/or enable new ones that were not feasible before due to the relatively slow imaging speed of conventional MRI. Work in progress includes fast implementation of CS reconstruction algorithms using parallel computing to enable the use of the combined approach in a clinical setting.

6. REFERENCES

[1] Candès E,Romberg J,Tao T. Robust uncertainty principles: Exact signal reconstruction from highly incomplete frequency information. IEEE Trans Inf Theory 2006;52(2):489-509.

[2] Donoho D. Compressed sensing. IEEE Trans Inf Theory 2006;52(4):1289-1306.

[3] Lustig M, Donoho D, Pauly JM. Sparse MRI: The application of compressed sensing for rapid MR imaging. Magn Reson Med. 2007;58(6):1182-95.

[4] Sodickson D. Manning W. Simultaneous acquisition of spatial harmonics (SMASH): fast imaging with radiofrequency coil arrays. Magn Reson Med. 1997; 38(4):591–603.

[5] Pruessmann KP, Weiger M, Scheidegger MB, Boesiger P. SENSE: sensitivity encoding for fast MRI. Magn Reson Med. 1999; 42(5):952-962.

[6] Griswold MA, Jakob PM, Heidemann RM, Nittka M, Jellus V, Wang J, Kiefer B, Haase A. Generalized autocalibrating partially parallel acquisitions (GRAPPA). Magn Reson Med. 2002; 47(6): 1202-10.

[7] Otazo R, Kim D, Axel L, Sodickson DK. Combination of compressed sensing and parallel imaging for highly accelerated first-pass cardiac perfusion MRI. Magn Reson Med. 2010;64(3):767-76.

[8] Feng L, Otazo R, Jung H, Jensen J, Ye JC, Sodickson DK, Kim D. Accelerated cardiac T2 mapping using breath-hold multiecho fast spin-echo pulse sequence with k-t FOCUSS. Magn Reson Med. 2011;65:1661-9.

[9] Kim D, Dyvorne HA, Otazo R, Feng L, Sodickson DK, Lee VS. Accelerated phase-contrast cine MRI using k-t SPARSE-SENSE. Magn Reson Med. 2011.

[10] Otazo R, Sodickson DK. Distributed compressed sensing for accelerated MRI. In Proceedings of the 17th Annual Meeting of ISMRM, Hawaii, 2008. p 378.

[11] Feng L, Chandarana H, Block T, Sodickson DK, Otazo R. Accepted for the 2012 ISMRM Conference.

[12] Fessler J, Sutton B. Nonuniform fast Fourier transforms using min-max interpolation. IEEE Trans. Signal Processing 2003;51(2):560-74.

[13] Chandarana H, Block TK, Rosenkrantz AB, Lim RP, Kim D, Babb JS, Kiefer B, Lee VS. Free-breathing radial 3D fat-suppressed T1-weighted gradient echo sequence. Invest Radiol. 2011;46(10):648-53.